A characterization of the molecular phenotype and inflammatory response of schizophrenia patient-derived microglia-like cells

Ormel, Paul R.; Boettcher, Chotima; Gigase, Frederieke A. J.; Missall, Roy D.; van Zuiden, Welmoed; Zapata, M. Camila Fernandez; Ilhan, Dilara; de Goeij, Michelle; Udine, Evan; Sommer, Iris E. C.

Published in:
Brain behavior and immunity

DOI:
10.1016/j.bbi.2020.08.012

Publication date:
2020

Brain, Behavior, and Immunity 90 (2020) 196–207

Contents lists available at ScienceDirect

Brain, Behavior, and Immunity

journal homepage: www.elsevier.com/locate/ybrbi

A characterization of the molecular phenotype and inflammatory response of schizophrenia patient-derived microglia-like cells

Paul R. Ormel[a,b,c], Chotima Böttcher[d], Frederieke A.J. Gigase[a], Roy D. Missall[a], Welmoed van Zuiden[a], M. Camila Fernández Zapata[d], Dilara Ilhan[b], Michelle de Goeij[b], Evan Udine[e], Iris E.C. Sommer[f], Josef Priller[d,g,h,i,j], Towfique Raj[e], René S. Kahn[a], Elly M. Hol[b,k], Lot D. de Witte[a,c,l,*]

[a] Department of Psychiatry, Icahn School of Medicine at Mount Sinai, New York, NY, USA
[b] Department of Translational Neuroscience, University Medical Center Utrecht Brain Center, Utrecht University, Utrecht, The Netherlands
[c] Department of Psychiatry, University Medical Center Utrecht Brain Center, Utrecht University, Utrecht, The Netherlands
[d] Department of Neuropsychiatry and Laboratory of Molecular Psychiatry, Charité-Universitätsmedizin Berlin, Berlin, Germany
[e] Department of Neuroscience, Icahn School of Medicine at Mount Sinai, New York, NY, USA
[f] Department of Neuroscience, University Medical Center Groningen, Groningen, The Netherlands
[g] Berlin Institute of Health, Berlin, Germany
[h] Deutsches Zentrum Für Neurodegenartive Erkrankungen (DZNE), Bonn, Germany
[i] Cluster of Excellence NeuroCure, Berlin, Germany
[j] University of Edinburgh and UK Dementia Research Institute, Edinburgh, UK
[k] Department of Neuroimmunology, Netherlands Institute for Neuroscience, An Institute of the Royal Netherlands Academy of Arts and Sciences, Amsterdam, The Netherlands
[l] Mental Illness Research, Education and Clinical Center (MIRECC), James J Peters VA Medical Center, Bronx, NY, USA

ARTICLE INFO

Keywords:
Schizophrenia
Immune system
Microglia
Monocytes
Subclusters
Mass cytometry
RNA-seq

ABSTRACT

Different lines of evidence support a causal role for microglia in the pathogenesis of schizophrenia. However, how schizophrenia patient-derived microglia are affected at the phenotypic and functional level is still largely unknown. We used a recently described model to induce patient-derived microglia-like cells and used this to analyze changes in the molecular phenotype and function of myeloid cells in schizophrenia. We isolated monocytes from twenty recent-onset schizophrenia patients and twenty non-psychiatric controls. We cultured the cells towards an induced microglia-like phenotype (iMG), analyzed the phenotype of the cells by RNA sequencing and mass cytometry, and their response to LPS. Mass cytometry showed a high heterogeneity of iMG in cells derived from patients as well as controls. The prevalence of two iMG clusters was significantly higher in schizophrenia patients (adjusted p-value < 0.001). These subsets are characterized by expression of ApoE, Ccr2, CD18, CD44, and CD95, as well as IRF8, $P2Y_{12}$, Cx3cr1 and HLA-DR. In addition, we found that patient-derived iMG show an enhanced response to LPS, with increased secretion of TNF-α. Further studies are needed to replicate these findings, to determine whether similar subclusters are present in schizophrenia patients *in vivo*, and to address how these subclusters are related to the increased response to LPS, as well as other microglial functions.

1. Introduction

Microglia are the main population of immune cells in the brain parenchyma and are part of the myeloid immune system. Microglia play a crucial role in initiating and controlling inflammatory responses, but are also critical to several neurodevelopmental processes, such as neurogenesis, synaptogenesis and synaptic pruning. Since these processes are thought to be compromised in schizophrenia (Berdenis van Berlekom et al., 2019; Feinberg, 1982), it is hypothesized that microglia contribute to schizophrenia pathogenesis (Tay et al., 2017). This hypothesis is supported by two recent *meta*-analyses on a large number of transcriptome studies that have been performed on *post mortem* cerebral

* Corresponding author at: Department of Psychiatry, Icahn School of Medicine at Mount Sinai, One Gustave L. Levy Place, Box 1230, New York, NY 10029-6574, USA.
E-mail address: lotje.dewitte@mssm.edu (L.D. de Witte).

https://doi.org/10.1016/j.bbi.2020.08.012
Received 22 November 2019; Received in revised form 28 July 2020; Accepted 12 August 2020
Available online 13 August 2020

cortex lysates of schizophrenia patients and controls (Gandal et al., 2018a,b). At the gene level, numerous well-known microglial genes were significantly and consistently downregulated, such as *CX3CR1, IRF8, TREM2* and *P2RY12*. Expression of other genes, such as *APOE,* was upregulated. Together, these results indicate that the phenotype of microglia is changed in schizophrenia cerebral cortex tissue. However, it remains unknown whether these changes reflect an intrinsic and potentially causal dysregulation in myeloid immune cells, similar to what has been observed for neurons using patient-derived neuron-like cells (Hoffman et al., 2017).

The goal of this study was to increase our understanding of the molecular phenotype and function of myeloid cells derived from schizophrenia patients. We used a recently established model to culture patient-derived microglia-like cells (iMG) *in vitro* (Leone et al., 2006; Ohgidani et al., 2015; Ryan et al., 2017), with minor adaptations. Monocytes were cultured with several factors that are also expressed in the central nervous system (CNS) and that have shown to be crucial for microglia development. After 10 days, the cells adopt a microglia-like phenotype, including a ramified morphology and increased expression of microglia markers (Leone et al., 2006; Ohgidani et al., 2015; Ryan et al., 2017). This approach has recently been applied to investigate microglia function in schizophrenia and revealed changes in elimination of synapses in schizophrenia-derived iMG (Sellgren et al., 2019). An advantage of this model over iPSC-derived microglia, which more closely resemble primary microglia at the transcriptome level (Abud et al., 2017; Douvaras et al., 2017), is the use of short-term cultures without reprogramming. This allows for the characterizations of the microglia-like cells to be performed all at once and probably reduces the pronounced batch effects previously described for iPSC-differentiated neuron-like cells (Hoffman et al., 2017).

We cultured iMG from twenty recent-onset patients with schizophrenia and twenty controls. The cells were analyzed using RNA sequencing as well as mass cytometry, a technique that can be used to investigate differences in protein expression profiles between subpopulations of cells (Böttcher et al., 2019). We first analyzed whether schizophrenia-derived iMG show changes in key myeloid markers, including the genes that were differentially expressed in *post mortem* brain tissue (Gandal et al., 2018a,b). We subsequently performed a hypothesis-free analysis to explore alterations in gene and single-cell protein expression, as well as their response to the inflammatory trigger LPS.

2. Methods

2.1. Blood samples

Patients with a recent-onset psychotic disorder and controls were recruited into the tissue bank of the University Medical Center (UMC) Utrecht. Blood samples were collected between 2014 and 2018 as part of the CONTROLS study and as part of the baseline assessment of a randomized controlled trial consisting of placebo-simvastatin administration to study the treatment effect of simvastatin in schizophrenia (Begemann et al., 2015). Inclusion criteria of the simvastatin study were: recent-onset of psychotic symptoms (< 3 years), diagnosis of a schizophrenia-spectrum disorder (DSM-IV 295.xx), age between 18 and 50 years. Exclusion criteria were: chronic use of glucocorticosteroids, statins, other lipid-lowering drugs, or non-steroidal anti-inflammatory drugs (NSAIDs), pregnancy or breastfeeding, active liver, kidney, or muscle disease. Healthy controls were recruited via advertisements on notice boards, newspapers and on social media. Inclusion criterion for the CONTROLS study was an age between 18 and 70 years, exclusion criteria were a psychiatric illness as determined with the Comprehensive Assessment of Symptoms and History (CASH) (Andreasen et al., 1992), a family history of psychiatric illness, chronic use of glucocorticosteroids, statins, other lipid-lowering drugs, or NSAIDs, pregnancy or breastfeeding, presence of diabetes mellitus or severe heart failure and liver enzyme-inducing medication. All subjects provided written informed consent for participation. The blood samples were collected in sodium-heparin tubes from which peripheral blood mononuclear cells (PBMCs) were enriched using a ficoll-Paque centrifugation protocol by the tissue bank within 24 h after blood withdrawal. The cells were subsequently frozen in 10% DMSO and stored in liquid nitrogen. For the current study, we matched twenty schizophrenia patients with twenty subjects from the CONTROLS study based on age, BMI, and sex. Demographics are shown in Table 1 and in more detail in Supplementary Table 1.

Table 1
Demographics of included donors.

	Controls	SCZ patients
N	20	20
Sex (female/male)	4/16	4/16
Age (mean ± STDEV)	25 ± 6	23 ± 4
BMI (mean ± STDEV)	25 ± 5	25 ± 4
RIN (mean ± STDEV)	9.0 ± 0.2	8.7 ± 1.4
Antipsychotic use (N)	0	18
hs-CRP (median + IQR)	1.95 (1–2.8)	2.15 (1–2.68)

BMI = body mass index; RIN = RNA integrity number; hs-CRP = high sensitivity.
C-reactive protein; STDEV = standard deviation; IQR = interquartile range.

2.2. Monocyte isolation and monocyte-derived microglia-like cell (iMG) differentiation

A vial with 10 million PBMCs was thawed and washed in monocyte culture medium without serum (RPMI 1640 (Life technologies, 21875034), 2 mM L- glutamine, 100 U/mL penicillin and 100 μg/mL streptomycin (BioWhittaker, Belgium)). The cells were seeded at a density of $1*10^6$ cells/well in poly-L lysine hydrobromide (PLL)-coated 48-well flat-bottom plates at 37 °C in 5% CO_2 for 2 h (h). Non-adhering cells (mostly lymphocytes) were removed by washing the wells with PBS (pH 7.4 Gibco Life technologies, MA). Monocyte culture medium +25% astrocyte-conditioned medium (ACM) (SCC1811, ScienCell, USA) was added to the wells and cells were cultured at 37 °C in 5% CO_2. On the fourth and eighth day of culture, cells were washed again and medium was replaced with monocyte-derived microglia (iMG) medium (RPMI 1640, 2 mM L- glutamine, 100 U/mL penicillin, 100 μg/mL streptomycin, 25% ACM, 10 ng/ml M−CSF, 10 ng/ml GM-CSF, 20 ng/ml TGFβ, 12.5 ng/ml IFNγ, and 100 ng/ml IL34 (all cytokines from Miltenyi Biotech, Germany)). This approach was based on a number of published protocols to generate microglia-like cells from monocytes to investigate disease-related microglia phenotypes, including schizophrenia (Etemad et al., 2012; Leone et al., 2006; Ohgidani et al., 2015; Ryan et al., 2017; Sellgren et al., 2019). These protocols apply different combinations of factors to differentiate monocytes towards microglia. This includes astrocyte-conditioned medium (Leone et al., 2006), or an extracellular matrix (Sellgren et al., 2019), as well as combinations with IL34, GM-CSF, M−CSF and other soluble factors important to microglia development (Etemad et al., 2012; Ohgidani et al., 2015; Ryan et al., 2017). We optimized our protocol based on the expression of *TREM2, TYROBP* and *PROS1*. The iMG cultures of 20 patients and 20 controls were performed all in one batch. To compare the phenotype of the cells with monocytes, we isolated these cells as described by us before (Ormel et al., 2017). Monocytes were positively selected from PBMCs by $CD14^+$ magnetic associated cell sorting (MACs) according to manufacturer's protocol (Miltenyi, Germany, 130-050-201). The cells were subsequently collected in fixation/stabilization buffer (SmartTube, USA, PROT1), or Trizol reagent (Life Technologies, 15596018) for subsequent protein or RNA purification, respectively.

2.3. Human microglia isolation

To characterize the phenotype of iMG we compared the transcriptome of the cells with monocytes and microglia isolated from *post mortem* brain tissue. Fresh *post mortem* brain tissue needed for the microglia samples was provided by the Netherlands Brain Bank (www.hersenbank.nl). All donors provided written consent during life. The tissue bank protocols and our study design were approved by the human ethics committee of the UMC Utrecht. Microglia were isolated as described by us before (Sneeboer et al., 2019). Human microglia (MG) were enriched from superior temporal gyrus (STG, n = 13) and medial frontal gyrus (MFG, n = 19) 2 to 24 h after autopsy. It was a mixed cohort of non-psychiatric controls (n = 17) and patients with different psychiatric disorders, but not schizophrenia (n = 15). The cohort consisted of 13 males and 19 females with an average age of 68.5 (± 20.4) years. By using mechanical dissociation together with enzymatic digestion (200 μg/mL DNAse 1 (Roche Diagnostics, 11284932001) and 3700 U/mL collagenase type 1 (Worthington, USA, LS004196)) a single-cell suspension was obtained. Myelin and red blood cells were removed by applying a Percoll (Amersham, Merck, Germany, 17-0891-01) gradient. Microglia were enriched by positive selection for CD11b expression by performing CD11b$^+$ (Miltenyi, USA, 130-049-601) MACs. The isolated cells were collected in Trizol reagent for subsequent RNA isolation.

2.4. RNA isolation, library preparation, and sequencing

RNA trizol samples were processed with the miRNeasy mini kit (Qiagen, The Netherlands, 217004) using manufacturer's protocol including the DNAse step (Qiagen, The Netherlands, 79254). The RNA concentration was determined using a VarioSkan Flash microplate reader (Thermo Scientific, MA). RNA integrity number (RIN) was assessed using the RNA 6000 Pico kit (Agilent Technology, USA, 5067-1513) and Agilent 2100 bioanalyzer according to manufacturer's protocol. cDNA synthesis and library preparation were performed with the SMART-Seq® v4 Ultra® Low Input RNA Kit (Takara Bio, USA, Inc., R634891, R634898, R638509) and the SMARTer® ThruPLEX® DNA-seq Kit (Takara Bio, USA, Inc., R400407) / Low Input Library Prep Kit v2 (Takara Bio, USA, Inc., 634899), respectively. Both according to manufacturer's protocol with an input of 5 ng RNA per sample. Shearing was performed using a Covaris AFA system and SPRI reagent (Beckman Coulter, USA) was subsequently used for the size selection of the fragmented cDNA (~500 bp per strand). Quantity and quality of the libraries were analyzed using the bioanalyzer. Three iMG and one monocyte did not pass this QC step and were excluded for further analyses. Samples were divided over several batches based on the sample molarity and pooled for sequencing on an illumina platform (illumina, USA).

2.5. RNAseq analysis

RNAseq reads were aligned along the GRCh38/hg38 reference genome via STAR aligner (Dobin et al., 2013) version 2.5 and genes were quantified using featureCounts (Liao et al., 2014). RNAseQC (Deluca et al., 2012) was used to calculate QC metrics using Rstudio (R version 3.5.3) and included: exonic rate, intergenic rate, mapped reads, rRNA rate, genes detected, and mean per base coverage. Principal component analyses and the variancePartition (Hoffman and Schadt, 2016) package (version 1.12.3) were used to detect potential outliers and to investigate potential confounders. All samples passed these QC steps and were included in subsequent analyses. Raw gene counts and transcript counts were normalized and differential expression was calculated with DESeq2 software (version 1.22.2) with an FDR < 0.05. Genes expressed in < 30% of the samples were excluded from analyses by using the cpm function of the edgeR package (version 3.24.3). The variance partition analysis revealed that gene expression was affected by batch, sex, and RIN values. We therefore corrected for these covariates whenever applicable in the analyses. The pheatmap package (version 1.0.12), visualizing differentially expressed genes (DGEs) with FDR < 0.05 was used to generate heatmaps of DGEs and expression of a microglia gene panel for characterization of the iMG model and to compare differences between patients and controls.

This microglia gene panel (Supplementary Table 3) was based on microglial signature genes (Patir et al., 2019) that were also differentially expressed in schizophrenia *post mortem* brain tissue (Gandal et al., 2018c). When comparing monocytes and iMG samples from the same individuals we used paired analyses based on subject ID. Gene ontology pathway analyses were performed with the GSEA online available tool of the BROAD institute (http://software.broadinstitute.org/gsea/index.jsp). Overlaps were computed using BioCarta gene sets, KEGG gene sets, and GO biological process. Plots were generated using enhanced volcano (version 1.1.3), ggplot2 (version 3.1.1.), and RColorBrewer (version 1.1.2).

2.6. Preparing samples for mass cytometry

Monocytes and iMG were fixed, stored, barcoded and stained for mass cytometry (CyTOF) as described by us before (Böttcher et al., 2019). Cells were collected in a 1.5 mL low binding Eppendorf (Sigma-Aldrich, The Netherlands, Z666505). They were fixed as a cell pellet in fixation/stabilization buffer (SmartTube, USA, PROT1) and stored at −80 °C until further use. Individual monocyte samples were thawed and stained with 89Y-CD45 (Fluidigm, USA, 3089003B) at 4 °C for 30 min. Cells were washed and monocytes and iMG from the same individual were pooled. Individual monocyte-iMG pooled samples were stained with premade combinations of six different palladium isotopes: ^{102}Pd, ^{104}Pd, ^{105}Pd, ^{106}Pd, ^{108}Pd & ^{110}Pd (Cell-ID 20-plex Pd Barcoding Kit, Fluidigm, USA, 201060). This multiplexing kit applies a 6-choose-3 barcoding scheme that results in 20 different combinations of three Pd isotopes. After 30 min staining (at room temperature/RT), individual samples were washed twice with cell staining buffer (0.5% bovine serum albumin in PBS, containing 2 mM EDTA). A total of 40 samples were pooled together, washed and further stained with antibodies in two separate batches. Anti-human antibodies were purchased either preconjugated to metal isotopes (Fluidigm, USA) or from commercial suppliers in purified form and conjugated in house using the MaxPar X8 kit (Fluidigm, USA, 201300) according to the manufacturer's protocol. Cells were re-suspended in 100 μL of antibody cocktail against surface markers (Supplementary Table 2) and incubated at 4 °C for 30 min. Then, cells were washed twice with cell staining buffer (0.5% bovine serum albumin in PBS, containing 2 mM EDTA). For intracellular staining, the stained cells were subsequently incubated in fixation/permeabilization buffer (Fix/Perm Buffer, eBioscience, USA, 88–8824-00) at 4 °C for 60 min. Cells were then washed twice with permeabilization buffer (eBioscience, USA, 00–8333-56). The samples were subsequently stained with antibody cocktails against intracellular molecules (Supplementary Table 2) in permeabilization buffer at 4 °C for 1 h. Cells were washed twice with permeabilization buffer and incubated in 4% methanol-free formaldehyde solution (Invitrogen, USA, R37814) overnight. Fixed cells were then washed and re-suspended in 1 mL iridium intercalator solution (Fluidigm, USA, 201192B) at RT for 1 h. Next, the samples were washed twice with cell staining buffer and then twice with ddH2O (Fluidigm, USA, 201069). Cells were pelleted and kept at 4 °C until CyTOF measurement. For compensating the CyTOF signal spillover, AbC total antibody compensation beads (Invitrogen, USA, A10513) were single stained with each of the antibodies used in the panel (Supplementary Table 2) according to manufacturer's instructions.

2.7. CyTOF measurement

Cells were analyzed using a CyTOF2 upgraded to Helios

specifications, with software version 6.7.1014 (Böttcher et al., 2019). The instrument was tuned according to the manufacturer's instructions with tuning solution (Fluidigm, USA, 201072). Measurement of EQ four element calibration beads (Fluidigm, USA, 201078) containing 140/142Ce, 151/153Eu, 165Ho, and 175/176Lu served as a quality control for sensitivity and recovery. Prior to analysis, cells were re-suspended in filtered ddH2O (20 μm Celltrix, Sysmex), counted, and adjusted to 3–5*10^5 cells/mL. EQ four element calibration beads were added at a final concentration of 1:10 v/v of the sample volume to be able to normalize the data to compensate for signal drift and day-to-day changes in instrument sensitivity. Samples were acquired with a flow rate of 300–400 events/second. Lower convolution threshold was set to 400, with noise reduction mode turned on and cell definition parameters set at event duration of 10–150 pushes (push = 13 μs). The resulting flow cytometry standard (FCS) files were normalized and randomized using the CyTOF software's internal FCS-Processing module on the non-randomized ('original') data. Settings were used according to the default settings in the software with time interval normalization (100 s/minimum of 50 beads) and passport version 2. Intervals with less than 50 beads per 100 s were excluded from the resulting FCS-file.

2.8. CyTOF data processing and analysis

Similar as in our previous study (Böttcher et al., 2019), we used Cytobank (www.cytobank.org) for initial manual gating on live single cells and boolean gating for de-barcoding. Nucleated single intact cells were manually gated according to DNA intercalators ^{191}Ir/^{193}Ir signals and event length. For de-barcoding, Boolean gating was used to deconvolute individual sample according to the barcode combination. All de-barcoded samples were then exported as individual FCS files for further analysis. Each FCS file was then compensated for signal spillover using R package CATALYST (Chevrier et al. 2018) and transformed with arcsinh transformation (scale factor 5) prior to data analysis. Immune phenotypes of monocytes and iMG were visualized using reduced-dimensional (2D) t-SNE maps generated according to the expression level of all markers used in the antibody panel. For embedding, we set hyperparameters to perplexity of 30, theta of 0.5, and iterations of 1,000 per 100,000 analysed cells). FCS files containing the t-SNE coordination as additional two parameters were exported from Cytobank for downstream exploratory and statistical analyses using R, as previously described (Böttcher et al., 2019; Nowicka et al., 2017). For population identification, *FlowSOM/Consensus ClusterPlus* (Chevrier et al., 2018; Nowicka et al., 2017; Van Gassen et al., 2015) clustering was used with 100 initial SOM-grid points and maxim of 25 *meta*-clusters. Based on visual inspection of t-SNE plots and heat maps, a final number of *meta*-clusters was chosen that divided clusters into populations with consistent phenotypes. We followed the concept of over-clustering, in order to study more specific populations at higher detail (Nowicka et al., 2017). The number of defined clusters may not solely represent biologically functional subsets in monocytes or iMG, but it should rather be interpreted as an exploratory tool for discovery of the differential abundance of small cell populations between the two studied groups (i.e. control vs patient).

2.9. LPS response

On day ten of differentiation we exposed iMG to 100 ng/mL lipopolysaccharide (LPS) derived from *Escherichia coli* (SigmaAldrich, USA, 0111:B4). After 6 h we harvested the cell culture supernatants as well as the cells that were lysed in Trizol reagent. The iMG stimulations of 20 patients and 20 controls were performed all in one batch. LPS stimulation of myeloid cells is known to induce expression of the cytokines IL1-beta, IL-6 and TNF-α. mRNA expression of *IL1B*, *IL6* and *TNF* was analyzed by quantitative PCR as described by us before (Ormel et al., 2017). Cytokine concentrations in the culture supernatants were determined by the human IL-6 and TNF-α ELISA kits of Invitrogen, according to the manufacturers protocol.

2.10. Phagocytosis assay

FluoSphere® Carboxylate-Modified Microspheres (2 μm, yellow-green fluorescent (505/515), 2% solids, ThermoFisher, F8827) were covalently coupled to human iC3b protein (Merck Millipore, 204863) according to manufacturer's protocol and as described by us before (Ormel et al., 2018). iMG were cultured with iC3b-coated or non-coated beads at a density of 3 beads/cell at 37 °C. After one hour, cells were washed three times with cold PBS to remove excess beads. Cells were subsequently detached by Trypsin 1X (10X, 15090, Thermofisher Scientific, USA) and EDTA (1:1000) (0.5 M, pH 8.0) for 6 min at 37 °C and collected with a cell scraper and analyzed by flow cytometry. Viable cells were selected by using forward and sideward scatterplots, and cells that phagocytized beads were gated and quantified by the FSC and the FL1 channel. To analyze the impact of microglial activation on phagocytosis capacity, the cells were stimulated with LPS 24 h prior to the phagocytosis assay.

2.11. Immunocytochemistry and microscopy

Monocytes were plated on PLL-coated coverslips in a 24-well flat-bottom plate. On day ten of differentiation, iMG were washed, fixed with 4% PFA, and immunostained for IBA1 (rabbit, Wako, 019-19741), and CD68 (mouse, Invitrogen, MA5-13324). After incubation with the secondary antibodies (donkey anti-rabbit, Alexa555, Abcam, 150074); donkey anti-mouse (Delight488, ThermoFisher, A21202)) and nuclear staining (hoechst, ThermoFisher, H3569), immunostainings were imaged with Zeiss Axio- Scope A1.

2.12. Statistics

Differential gene statistical analyses were performed in R (version 3.5.3) (CRAN: https://www.r-project.org) using a *p*-value adjustment (padj) to account for multiple testing with the Benjamini-Hochberg procedure. For the CyTOF analyses, data processing and analysis, as well as statistical testing were carried out in an unsupervised manner, to exclude the possibility of biased readouts. Analyses of statistical significance were performed by computational analysis using generalized linear mixed-effects model (GLMM) available through R package *diffcyt* and false discovery rate (FDR) adjustment (at 0.1 using Benjamini-Hochberg procedure) for multiple hypothesis testing. A p-value < 0.05 (unadjusted) at 0.1 FDR was considered statistically significant. Case-control differences for the response of iMG to LPS were analyzed with a Mann-Whitney *U* test, as data were not normally distributed. A *p*-value < 0.05 was considered statistically significant.

3. Results

3.1. Characterization of the monocyte-derived microglia-like cells (iMG) model.

Culturing monocytes for 10 days with a combination of factors important for microglia development induced a microglia-like ramified morphology and expression of microglia-markers CD68 and IBA1 (Fig. 1A, B). These iMG had a distinct protein expression profile compared to monocytes as shown by a separate clustering by single-cell mass cytometry (Fig. 1C), with heterogeneous expression of HLA-DR, IRF8 and CD95 (Supplementary Fig. 1A). Similar to microglia, ApoE was higher expressed in iMG than in monocytes (Fig. 1D,E). Most other proteins in our CyTOF panel had lower expression in iMG (Supplementary Fig. 1B). This was true for markers that are higher expressed in monocytes *in vivo*, such as CCR2 and CD36, but also for markers that have higher expression in acutely isolated microglia compared to monocytes, including $P2Y_{12}$ (Fig. 1D, E; Supplementary

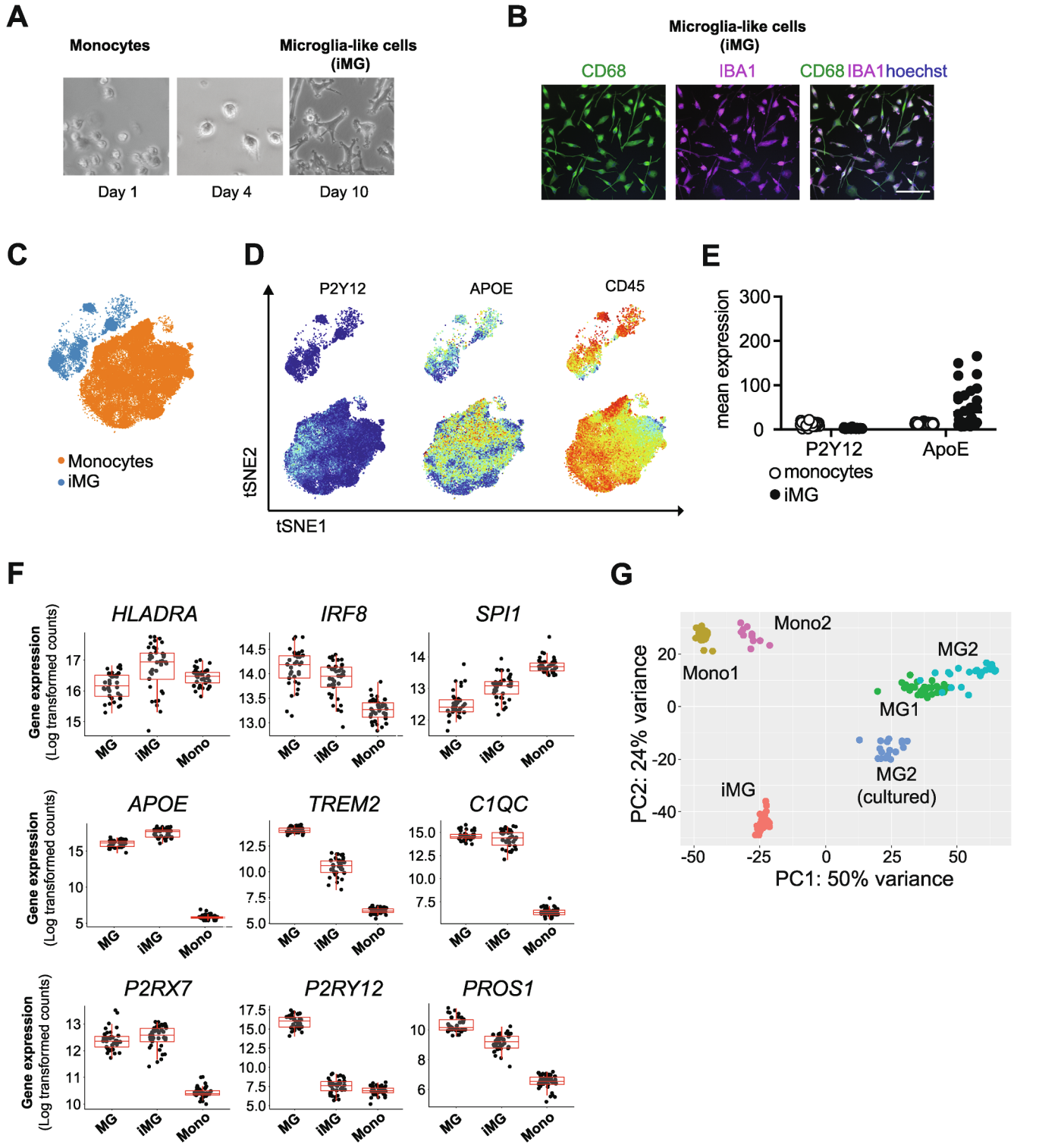

Fig. 1. Characterization of monocyte-derived microglia-like cells (iMG). A) Representative images of morphological transformation during differentiation of monocytes into monocyte-derived microglia-like cells (iMG). B) CD68 and IBA1 immunostainings of iMG together with a nuclear staining (hoechst). Scale bar is 40 μm. C) Representative reduced-dimensional single-cell t-SNE maps of a paired iMG (blue) and monocyte sample (orange). Each dot represents one cell. The 2D t-SNE maps were generated based on expression levels of all analyzed markers. D) t-SNE plots show expression levels of markers in iMG (top) and monocytes (bottom). The color spectrum represents individual marker-expression levels (red, high expression; dark blue, low expression). E) Dotplots of $P2Y_{12}$ and ApoE expression of all monocyte and iMG samples as determined by mass cytometry. F) Dotplots of expression of microglia genes depicting vst log transformed counts between monocytes (Mono), iMG, and human primary microglia (MG) isolated from *post mortem* brain material. G) Principal component analysis (PCA) on vst log transformed counts of our monocytes (Mono1), iMG, primary human microglia (MG1) isolated and sequenced in our lab, as well as transcriptome data of Gosselin et al. (2017) on monocytes (Mono2), human MG (MG2), and human MG that have been in culture for 7 till 10 days (MG2, cultured). (For interpretation of the references to color in this figure legend, the reader is referred to the web version of this article.)

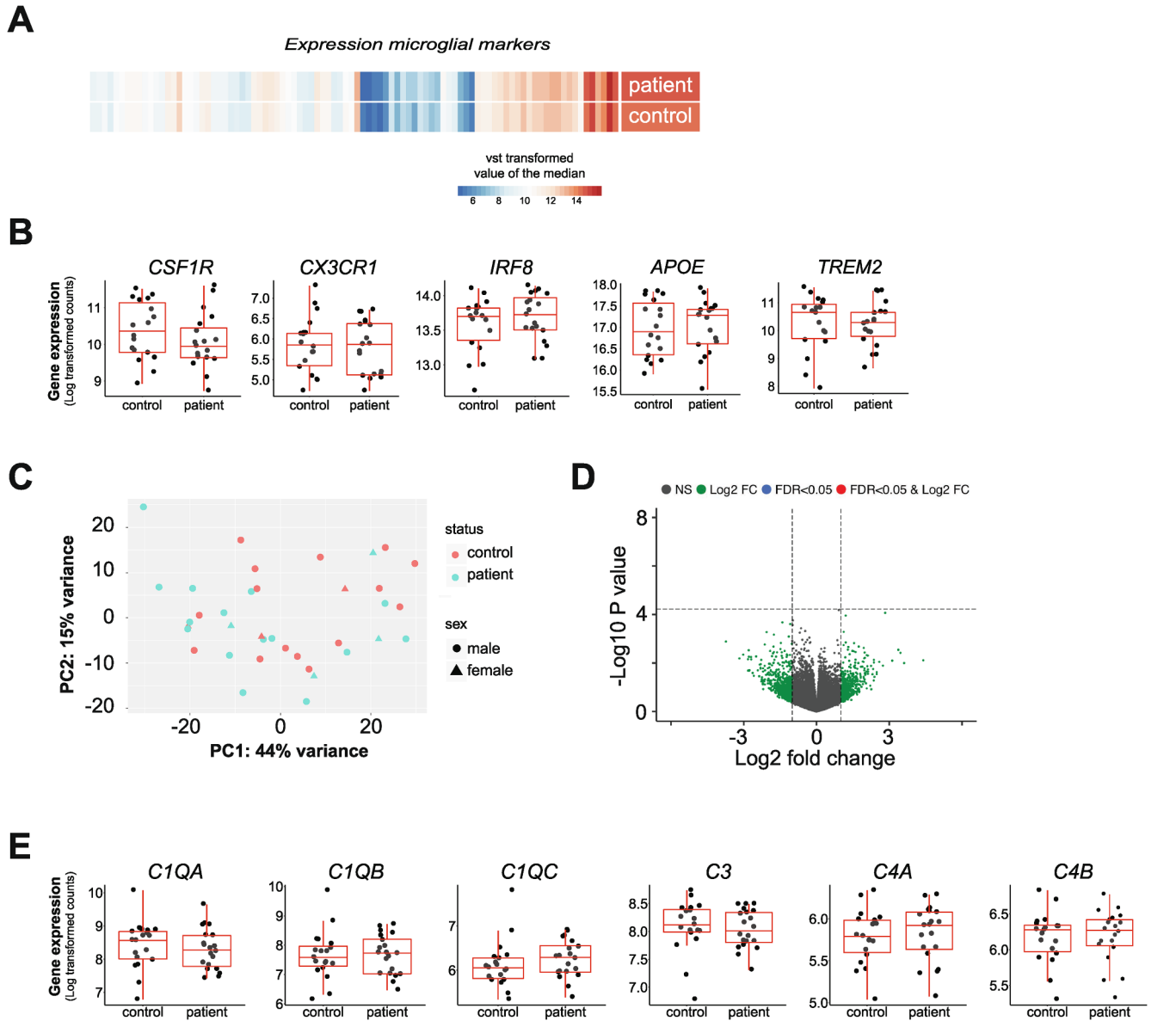

Fig. 2. Gene expression analysis of iMG of schizophrenia patients compared to controls. iMG were generated from monocytes isolated from twenty patients with schizophrenia and twenty controls and RNA sequencing was performed to analyze changes in gene expression. Significance was determined using DESeq2 with a p-value adjustment (padj) to account for multiple testing with the Benjamini-Hochberg procedure. A) Heatmap representation of unsupervised clustered expression of vst log transformed counts of a panel of microglia signature genes. The medians per gene of patients and controls were used for the heatmap. B) Dotplots depicting expression levels of *CSF1R, CX3CR1, IRF8, TREM2,* and *APOE.* C) PCA on vst log transformed counts of genes. D) Volcano plots showing differential gene expression (DGE) between samples from patients and controls. E) Dotplots depicting expression levels of *C1QA, C1QB, C1QC, C3, C4A* and *C4B.*

Fig. 1B). Whole transcriptome analysis showed a distinct transcriptome profile of iMG compared to monocytes with 21,630 differentially expressed genes (DGE) with an FDR $<$ 0.05 and an upregulation of lysosomal and complement pathways in iMG (Supplementary Fig. 2A, B). To further characterize the iMG phenotype, we also compared gene expression data of primary human microglia (MG). Expression levels of several well-known microglia genes, such as *APOE*, *TREM2*, *C1QA-C*, *IRF8 and P2RX7* were similar between iMG and primary MG. However, other microglial markers, including *P2RY12*, were not upregulated in iMG compared to monocytes (Fig. 1E, F). Comparative analyses including transcriptome data from a previous study (Gosselin et al., 2017) showed that primary microglia that were cultured for 7–10 days (MG2 cultured) clustered more closely to iMG in a PCA than our (Mono1) and their monocytes (Mono2), and our and their primary microglia acutely harvested (MG2) (Fig. 1G). Unsupervised clustering based on expression of a microglia-related gene panel showed that MG2 (cultured) clustered with iMG before clustering with other cell types (Supplementary Fig. 2C). At the functional level, lipopolysaccharide (LPS) exposure of iMG resulted, as expected, in immune activation (Supplementary Fig. 3A-C). In addition, the cells mediate phagocytosis of fluorescent beads and this is increased when the beads are coated with the complement component iC3b and after the cells have been stimulated with LPS (Supplementary Fig. 4A-D)

3.2. Gene expression analysis of iMG derived from monocytes of patients and controls.

We first analyzed whether iMG derived from schizophrenia patients show changes in the expression of a panel of microglia signature genes (Patir et al., 2019), which are differentially expressed in schizophrenia-derived bulk *post mortem* brain tissue (Gandal et al., 2018b). iMG, cultured from twenty patients and twenty controls (Table 1), did not

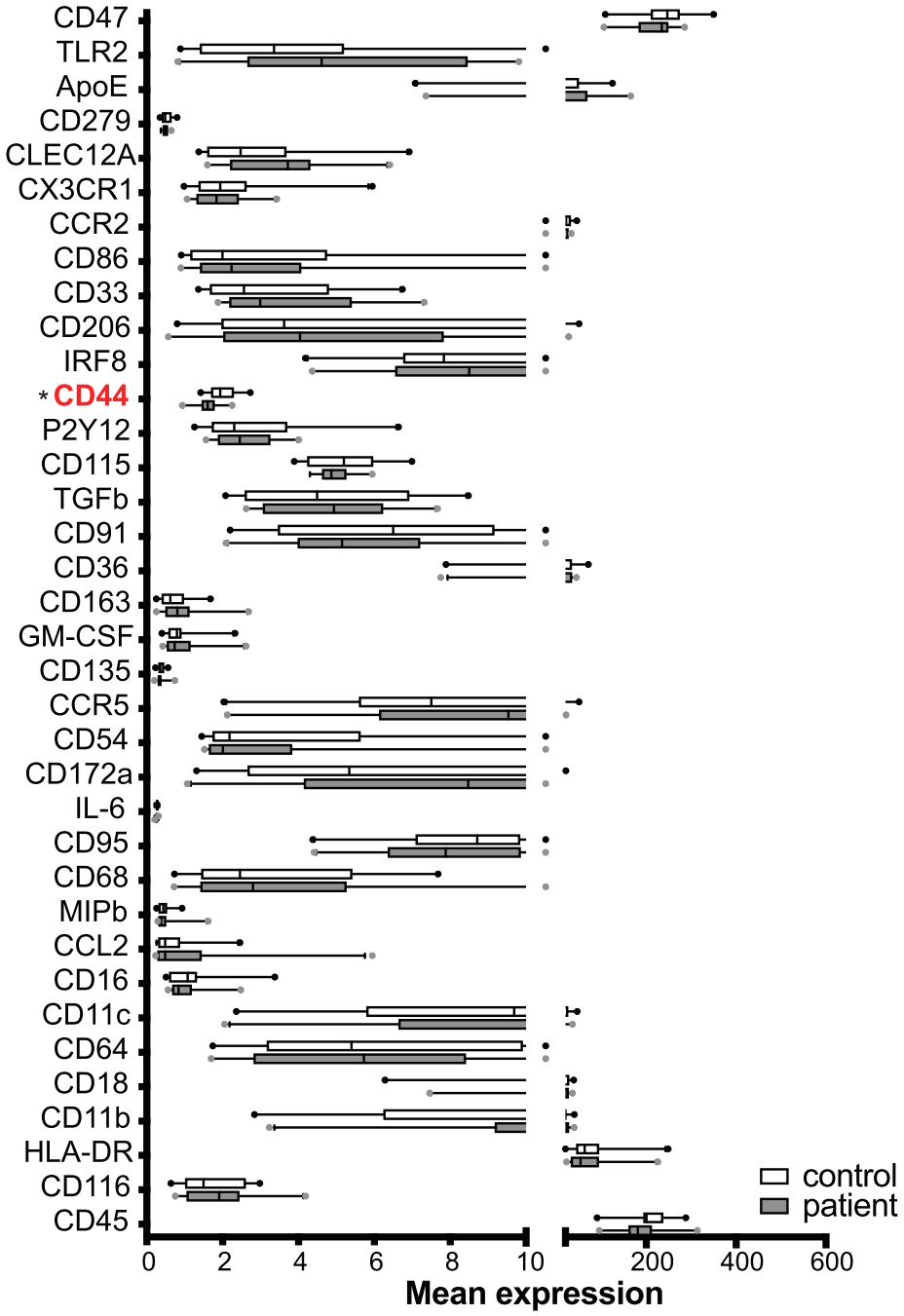

Fig. 3. Protein expression of iMG compared between patients and controls. iMG were generated from monocytes isolated from twenty patients with schizophrenia and twenty controls and analyzed by mass cytometry to analyze changes in a panel of 36 proteins. Boxplots show mean and standard deviation of protein expression levels. Asterisk indicates differentially expressed protein (padj $<$ 0.05).

show differential expression of any genes in this panel, including, *CSF1R, CX3CR1, IRF8, APOE and TREM2* (Fig. 2A-B). We continued with a hypothesis-free approach and analyzed differential gene expression (DGE) between iMG derived from patients and controls. A principle component analysis (PCA) did not separate patients from controls (Fig. 2C), and we did not detect any differentially expressed genes (Fig. 2D; extended data file). This includes the C1Q, C3 and C4 complement genes, that are involved in mediating synaptic pruning by microglia (Stevens et al., 2007), a process that has been associated with schizophrenia through genetic studies (Sekar et al., 2016)

3.3. Protein expression analysis

Next, we compared expression of a panel of 36 proteins in the iMG samples between cases and controls. Expression of CD44 was significantly downregulated (Fig. 3). None of the other proteins was differentially expressed. We subsequently analyzed whether we observed differences in the frequencies of clusters of iMGs between patients and controls. Clustering analysis of iMG recognized 15 clusters (Fig. 4A, B). Clusters #6 and #15 had a significantly higher abundance in patients with schizophrenia (Fig. 4C-D, padj $<$ 0.001). These clusters expressed higher levels of ApoE, Ccr2, CD18, CD44, and CD95 compared to other clusters (Fig. 4E). Furthermore, cluster #6 (cl-6) expressed higher levels of human microglia/macrophage markers such as CD11b, CD115,

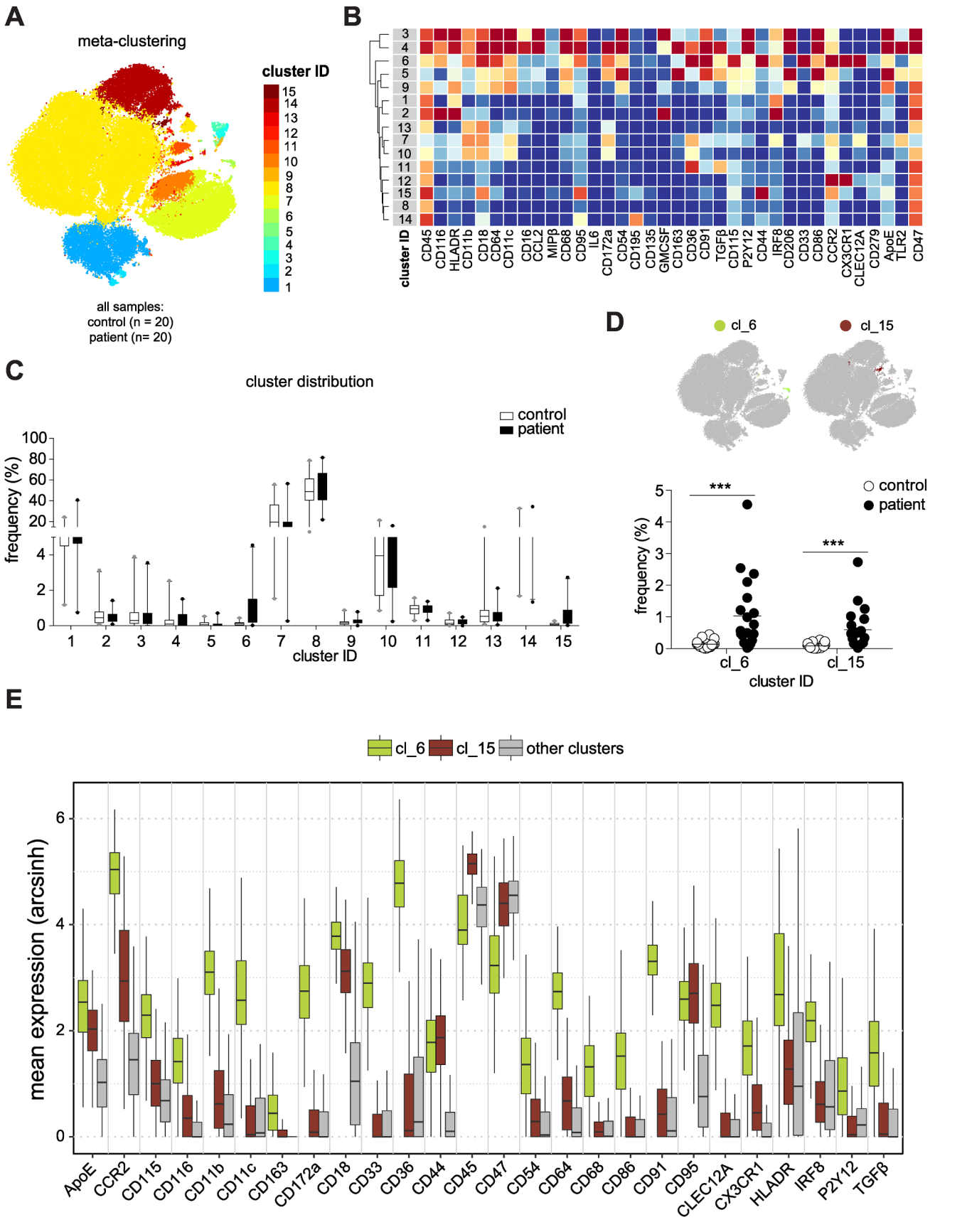

(caption on next page)

Fig. 4. Differential abundances of iMG cell subsets in patients with schizophrenia. iMG were generated from monocytes isolated from 20 patients with schizophrenia and 20 controls and analyzed by mass cytometry. A) t-SNE map of concatenated FCS files from all 40 iMG samples. The coloring indicates fifteen defined clusters of iMG; B) Heat map and cluster analysis of all samples demonstrating the phenotypes of all 15 defined clusters on the basis of the mean expression levels of 36 markers used for the cluster analysis. Identified clusters are indicated by dendrograms. Heat colors show overall marker expression levels (red, high expression; dark blue, no expression). C) Boxplots showing frequencies of each defined clusters in patients versus controls; D) t-SNE maps showing the differentially abundant cluster #6 (light green) and abundant cluster #15 (merlot). Dotplot (lower panel) depicting differences in frequency (%) of the two differentially abundant clusters (#6 and #15) between control individuals (control, white dots) and patients with schizophrenia (patient, black dots) Asterisk indicates differentially expressed protein (*** = padj < 0.001).; E) Boxplots of mean and standard deviation of protein expression for randomly selected cells in the cluster 6 (green, n = 256), 15 (merlot, n = 256) and all other clusters (grey, n = 256). All twenty-six markers were statistically detected as markers defining the differentially abundant cluster 6 and 15. (For interpretation of the references to color in this figure legend, the reader is referred to the web version of this article.)

CD11c, CD172a, CD64, CD68, Cx3cr1, HLA-DR, IRF-8, $P2Y_{12}$, and TGF-β1, whereas expression of CD45 and CD47 were lower than in other clusters. Next, we analyzed whether similar changes were detected also in undifferentiated monocytes. We found a high homogeneity in single-cell monocyte phenotype (Supplementary Fig. 5A), and no differences in cellular heterogeneity (i.e. cluster distribution) between patients and controls (Supplementary Fig. 5B).

3.4. Inflammatory responses

To assess the inflammatory response of iMG, we analyzed the response of the cells to stimulation with lipopolysaccharide (LPS) for six hours. LPS is known to induce a robust upregulation of expression of pro-inflammatory cytokines, such as IL1-beta, IL-6 and TNF-α. mRNA expression of these cytokines at baseline showed a trend towards upregulation, but this was not significant (*IL1B U* 153, *p*-value 0.21; *IL6 U* 127, *p*-value 0.13; *TNF U* 141, *p*-value 0.17) (Fig. 5A). Stimulation of the cells with LPS resulted in a strong upregulation of expression of these genes (Fig. 5B). Expression after stimulation showed the same trend towards upregulation in schizophrenia patients, but again not significant (*IL1B U* 148, *p*-value 0.67; *IL6 U* 125, *p*-value 0.17; *TNF U* 121, *p*-value 0.13) (Fig. 5C). Stimulation also resulted in the upregulation of IL-6 and TNF-α protein secretion (Fig. 5D). TNF-α protein secretion was significantly higher in patients (*U* 117.5, *p*-value 0.043), IL-6 showed the same trend, but results were not significant (*U* 136, *p*-value 0.13).

4. Discussion

The goal of this study was to increase our understanding of the phenotype and function of microglia in schizophrenia. At the transcriptome level we did not find differences between iMG from patients and controls. This includes inflammatory genes, complement or phagocytosis-related genes, as well as microglial signature genes (Patir et al., 2019) that are differentially expressed in brain tissue of schizophrenia patients (Gandal et al., 2018b). These data suggest that the changes observed in expression of microglial genes in bulk *post mortem* tissue are caused by specific changes in schizophrenia brain tissue rather than endogenous, potentially genetic, alterations in all myeloid cells. This is in accordance with the limited number of genetic risk variants for schizophrenia that can be related to immune- and specifically microglial pathways (Skene et al., 2018; van Mierlo et al., 2020). Furthermore, we did not find changes in complement genes, which could be involved in the functional phenotype recently described in monocyte-derived microglia of schizophrenia patients (Sellgren et al., 2019).

To study more specific subpopulations at higher detail, we took advantages of unbiased algorithm-based analyses, which allowed an investigation of rare cell populations. Specifically, we followed the concept of over-clustering for second-level *meta*-clustering of iMG. The number of defined clusters may not solely represent biologically functional subsets in each cell population, but it should rather be interpreted as an exploratory tool for discovery of differential abundances of small cell populations between the two studied groups. We were able to distinguish various iMG subpopulations using a panel of 36 myeloid proteins. Two of the smaller subpopulations identified with this method were unique to iMG derived from patients with schizophrenia. These clusters showed increased expression of key microglia proteins, such as Cx3cr1, IRF-8, ApoE and $P2Y_{12}$, but also higher expression of other markers such as CD18, CD44, Ccr2, CD18 and CD95. It is important to note that a high expression of CD18, CD44, Ccr2 and Cx3cr1 has also been described for bone-marrow derived $CD14^+CD16^+$ monocytes (Mandl et al., 2014). However, in undifferentiated monocytes we did not detect similar changes in subclusters of cells. These data suggest that there may be differences in regulatory pathways important for myeloid cell survival, differentiation and potentially microglia development in schizophrenia. Whether a unique microglia population is also present in schizophrenia brain tissue or whether our findings reflect an artefact of our differentiation protocol requires further investigation, such as single-cell/nuclei RNAseq on whole brain tissue from patients with schizophrenia. In addition, it will be interesting to determine whether similar subclusters of microglia are detected in animal models of schizophrenia, such as the Maternal Immune Activation (MIA) model, where phenotypic changes of microglia are consistently found (Mattei et al., 2017).

Our analysis of the inflammatory response of iMG suggests a stronger response of the cells to the TLR-4/CD14 ligand LPS in schizophrenia patients, which was most apparent for the secretion of TNF-α protein. Increased levels of peripheral TNF-α and IL-6 have been repetitively found for schizophrenia (Hoseth et al., 2017; Upthegrove et al., 2014). LPS-activated monocytes from schizophrenia were found to express increased TNF-α in a previous study (Kowalski et al., 2001), but not by a more recent study (Krause et al., 2012). Our results in iMG are suggestive of an enhanced response of microglia to inflammatory triggers in schizophrenia. Cytokines, such as TNF-α and IL-6, play an important role in the cross-talk between microglia and neurons. This cross-talk has been shown to be crucial for the regulation of several neurodevelopmental and physiological neuronal processes, such as neurogenesis, synaptogenesis, synaptic pruning, synaptic scaling and neurotransmission (Lewitus et al., 2016; Stellwagen and Malenka, 2006; Werneburg et al., 2017). A dysregulation of the production of these cytokines may therefore affect these neurodevelopmental processes which are thought to be involved in schizophrenia pathogenesis.

In addition to our case-control comparison, we provided an in-depth characterization of the iMG model. As previously reported, we showed that iMG have a microglia-like morphology and perform key myeloid functions, including inflammatory responses and phagocytosis. Monocytes and iMG have a distinct mRNA and protein expression profile. Expression of some markers resembles the levels in primary microglia, such as *C1QA-C* and *APOE*. This indicates that our 'artificial CNS environment' provided cues important for inducing the microglia-like phenotype. However, we also show that this was not the case for markers such as $P2Y_{12}$. Many of the genes that were downregulated in iMG compared to primary microglia, are also downregulated when primary microglia are cultured after isolation from brain tissue (Gosselin et al., 2017). To fully mimic a microglia cell, iMG are likely dependent on direct contact with neurons and other brain cell types and the result of the distinct early hematopoietic development described for primary microglia (Ginhoux et al., 2010).

The strengths of this study are the in-depth profiling of myeloid cells

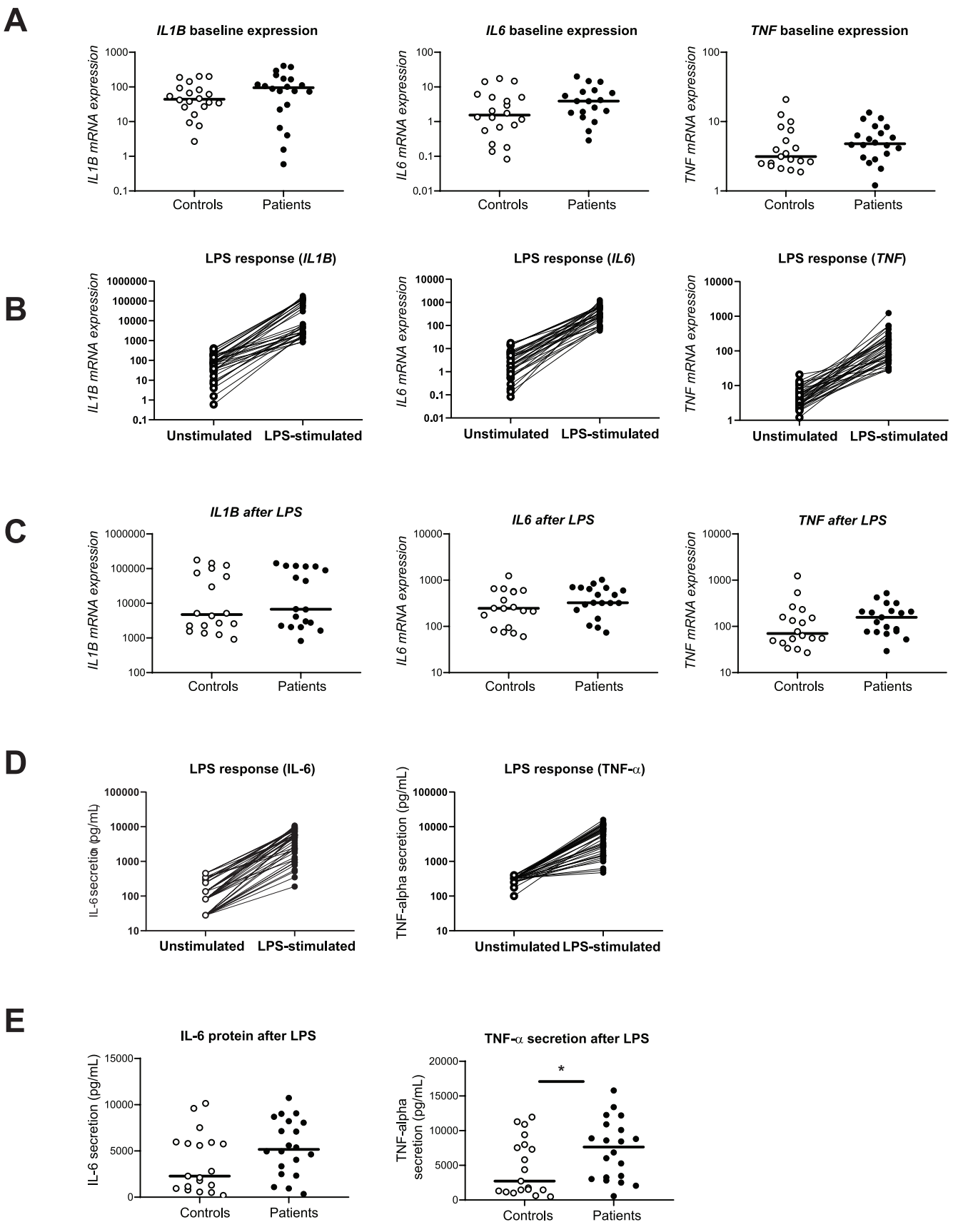

(caption on next page)

Fig. 5. Comparison of the LPS response of iMG between patients and controls. iMG were stimulated with lipopolysaccharide (LPS) for 6 h. mRNA expression of *IL1B*, *IL6* and *TNF* was measured by quantitative PCR (qPCR). A) shows the expression of unstimulated samples; B) the change in expression after LPS stimulation and C) the expression of the LPS-stimulated samples of patients and controls. Every dot represents one donor and the line shows the median. Cytokine secretion of IL6 and TNF-α was measured by ELISA on the culture supernatants. D) shows the IL-6 and TNF-α response of iMG to LPS and E) the levels of these cytokines in in LPS-stimulated iMG of patients and controls. Every dot represents one donor and the median is depicted. Case-control differences in A, B, C and E were determined with a Mann-Whitney *U* test. * = p-value < 0.05.

from patients with recent-onset schizophrenia and well-matched controls; and the combination of a hypothesis-driven as well as unbiased analysis of the data. By applying mass cytometry, we were also able to investigate changes in subclusters of iMG that were undetectable at the level of bulk protein analysis. The current study also has limitations. First, taking into account the heterogeneity of schizophrenia, a larger cohort would have provided more power to detect smaller effect sizes or changes in subgroups of patients. Secondly, although we were able to induce microglia-like features, monocytes are not the natural progenitors of *in vivo* microglia and the cells therefore still lack part of the microglia phenotype, which we have characterized in this paper. Lastly, although we matched the groups and regressed out effects caused by sex, BMI, and technical covariates, we were unable to control for every potential confounder, such as coffee, smoking and antipsychotic use. Several lines of evidence indicate that antipsychotics may have an impact on myeloid cells, possibly with reduction of inflammatory capacities (Baumeister et al., 2016; Cotel et al., 2015; Kato et al., 2011). Since 18/20 patients in our study used medication at the time of monocyte isolation, we checked the expression of *IL1B*, *IL6* and *TNF* in undifferentiated monocytes. We did not find a decreased expression of these cytokines (data not shown). Also, we cultured the iMG for 10 days without antipsychotics, and we found enhanced inflammatory responses in schizophrenia-derived iMG. Nevertheless, our iMG results should be repeated using monocytes from drug-naïve first-episode patients to rule out a potential effect of antipsychotics.

In conclusion, our results provide indications for alterations in developmental pathways of microglia, as well as an altered response of schizophrenia-derived myeloid cells to inflammatory triggers in schizophrenia. Replication of the results in iMG and iPSC-derived microglia are needed as well as follow-up studies in animals or *in vitro* co-culture systems to understand the consequences of these phenotypes.

Acknowledgements

This study was funded by a TOP subsidy (91212154) of The Netherlands Organization for Health Research and Development (ZONMW) and the German Research Foundation (SFB TRR167 B05). We thank the patients and control subjects for participating in this study. We thank Marjolein Sneeboer for isolating the microglia samples. We are grateful to the Netherlands Brain Bank for their excellent services (www.hersenbank.nl). We thank the group of Prof. dr. M. Merad and specifically Fiona Desland for setting up the ultra-low input RNA library preparation. We are grateful for the support of the research team of the simvastatin and CONTROLS study and especially Marieke Begemann, Shiral S. Gangadin, Maya Schutte and Neeltje van Haren. We thank Fokke Terpstra and the tissue bank for their support in collecting the samples. Lastly, we are grateful for the advice on bioinformatics from K. Van Eijk and R. Zwamborn.

Appendix A. Supplementary data

Supplementary data to this article can be found online at https://doi.org/10.1016/j.bbi.2020.08.012.

References

Abud, E.M., Ramirez, R.N., Martinez, E.S., Healy, L.M., Nguyen, C.H.H., Newman, S.A., Yeromin, A.V., Scarfone, V.M., Marsh, S.E., Fimbres, C., Caraway, C.A., Fote, G.M., Madany, A.M., Agrawal, A., Kayed, R., Gylys, K.H., Cahalan, M.D., Cummings, B.J., Antel, J.P., Mortazavi, A., Carson, M.J., Poon, W.W., Blurton-Jones, M., 2017. iPSC-derived human microglia-like cells to study neurological diseases. Neuron 94 (2), 278–293.e9.

Andreasen, N.C., Flaum, M., Arndt, S., 1992. The Comprehensive Assessment of Symptoms and History (CASH). An instrument for assessing diagnosis and psychopathology. Arch. Gen. Psychiatry 49, 615–623. https://doi.org/10.1001/archpsyc.1992.01820080023004.

Baumeister, D., Ciufolini, S., Mondelli, V., 2016. Effects of psychotropic drugs on inflammation: consequence or mediator of therapeutic effects in psychiatric treatment? Psychopharmacology (Berl). https://doi.org/10.1007/s00213-015-4044-5.

Begemann, M.J.H., Schutte, M.J.L., Slot, M.I.E., Doorduin, J., Bakker, P.R., van Haren, N.E.M., Sommer, I.E.C., 2015. Simvastatin augmentation for recent-onset psychotic disorder: a study protocol. BBA Clin. https://doi.org/10.1016/j.bbacli.2015.06.007.

Berdenis van Berlekom, A., Muflihah, C.H., Snijders, G.J.L.J., MacGillavry, H.D., Middeldorp, J., Hol, E.M., Kahn, R.S., de Witte, L.D., 2019. Synapse pathology in schizophrenia: a meta-analysis of postsynaptic elements in postmortem brain studies. Schizophr. Bull. https://doi.org/10.1093/schbul/sbz060.

Böttcher, C., Schlickeiser, S., Sneeboer, M.A.M., Kunkel, D., Knop, A., Paza, E., Fidzinski, P., Kraus, L., Snijders, G.J.L., Kahn, R.S., Schulz, A.R., Mei, H.E., Hol, E.M., Siegmund, B., Glauben, R., Spruth, E.J., de Witte, L.D., Priller, J., 2019. Human microglia regional heterogeneity and phenotypes determined by multiplexed single-cell mass cytometry. Nat Neurosci 22, 78–90. https://doi.org/10.1038/s41593-018-0290-2.

Chevrier, S., Crowell, H.L., Zanotelli, V.R.T., Engler, S., Robinson, M.D., Bodenmiller, B., 2018. Compensation of signal spillover in suspension and imaging mass cytometry. Cell Syst. https://doi.org/10.1016/j.cels.2018.02.010.

Cotel, M.-C., Lenartowicz, E.M., Natesan, S., Modo, M.M., Cooper, J.D., Williams, S.C.R., Kapur, S., Vernon, A.C., 2015. Microglial activation in the rat brain following chronic antipsychotic treatment at clinically relevant doses. Eur. Neuropsychopharmacol. https://doi.org/10.1016/j.euroneuro.2015.08.004.

Deluca, D.S., Levin, J.Z., Sivachenko, A., Fennell, T., Nazaire, M.D., Williams, C., Reich, M., Winckler, W., Getz, G., 2012. RNA-SeQC: RNA-seq metrics for quality control and process optimization. Bioinformatics. https://doi.org/10.1093/bioinformatics/bts196.

Dobin, A., Davis, C.A., Schlesinger, F., Drenkow, J., Zaleski, C., Jha, S., Batut, P., Chaisson, M., Gingeras, T.R., 2013. STAR: ultrafast universal RNA-seq aligner. Bioinformatics 29, 15–21. https://doi.org/10.1093/bioinformatics/bts635.

Douvaras, P., Sun, B., Wang, M., Kruglikov, I., Lallos, G., Zimmer, M., Terrenoire, C., Zhang, B., Gandy, S., Schadt, E., Freytes, D.O., Noggle, S., Fossati, V., 2017. Directed differentiation of human pluripotent stem cells to microglia. Stem Cell Reports 8, 1516–1524. https://doi.org/10.1016/j.stemcr.2017.04.023.

Etemad, S., Zamin, R.M., Ruitenberg, M.J., Filgueira, L., 2012. A novel in vitro human microglia model: Characterization of human monocyte-derived microglia. J. Neurosci. Methods. https://doi.org/10.1016/j.jneumeth.2012.05.025.

Feinberg, I., 1982. Schizophrenia: Caused by a fault in programmed synaptic elimination during adolescence? J. Psychiatric Res.

Gandal, M.J., Haney, J.R., Parikshak, N.N., Leppa, V., Ramaswami, G., Hartl, C., Schork, A.J., Appadurai, V., Buil, A., Werge, T.M., Liu, C., White, K.P., Horvath, S., Geschwind, D.H., 2018a. Shared molecular neuropathology across major psychiatric disorders parallels polygenic overlap. Science 359 (6376), 693–697.

Gandal, M.J., Zhang, P., Hadjimichael, E., Walker, R.L., Chen, C., Liu, S., Won, H., van Bakel, H., Varghese, M., Wang, Y., Shieh, A.W., Haney, J., Parhami, S., Belmont, J., Kim, M., Moran Losada, P., Khan, Z., Mleczko, J., Xia, Y., Dai, R., Wang, D., Yang, Y.T., Xu, M., Fish, K., Hof, P.R., Warrell, J., Fitzgerald, D., White, K., Jaffe, A.E., Peters, M.A., Gerstein, M., Liu, C., Iakoucheva, L.M., Pinto, D., Geschwind, D.H., 2018. Transcriptome-wide isoform-level dysregulation in ASD, schizophrenia, and bipolar disorder. Science 362, eaat8127. https://doi.org/10.1126/science:aat8127.

Ginhoux, F., Greter, M., Leboeuf, M., Nandi, S., See, P., Gokhan, S., Mehler, M.F., Conway, S.J., Ng, L.G., Stanley, E.R., Samokhvalov, I.M., Merad, M., 2010. Fate mapping analysis reveals that adult microglia derive from primitive macrophages. Science 330, 841–845. https://doi.org/10.1126/science.1194637.

Gosselin, D., Skola, D., Coufal, N.G., Holtman, I.R., Schlachetzki, J.C.M., Sajti, E., Jaeger, B.N., O'Connor, C., Fitzpatrick, C., Pasillas, M.P., Pena, M., Adair, A., Gonda, D.D., Levy, M.L., Ransohoff, R.M., Gage, F.H., Glass, C.K., 2017. An environment-dependent transcriptional network specifies human microglia identity. Science 356. https://doi.org/10.1126/science:aal3222.

Hoffman, G.E., Hartley, B.J., Flaherty, E., Ladran, I., Gochman, P., Ruderfer, D.M., Stahl, E.A., Rapoport, J., Sklar, P., Brennand, K.J., 2017. Transcriptional signatures of schizophrenia in hiPSC-derived NPCs and neurons are concordant with post-mortem adult brains. Nat. Commun. 8. https://doi.org/10.1038/s41467-017-02330-5.

Hoffman, G.E., Schadt, E.E., 2016. variancePartition: interpreting drivers of variation in complex gene expression studies. BMC Bioinformatics. https://doi.org/10.1186/s12859-016-1323-z.

Hoseth, E.Z., Ueland, Thor, Dieset, I., Birnbaum, R., Shin, J.H., Kleinman, J.E., Hyde, T.M., Mørch, R.H., Hope, S., Lekva, T., Abraityte, A.J., Michelsen, A.E., Melle, I., Westlye, L.T., Ueland, Torill, Djurovic, S., Aukrust, P., Weinberger, D.R., Andreassen,

O.A., 2017. A study of TNF pathway activation in schizophrenia and bipolar disorder in plasma and brain tissue. Schizophr. Bull. https://doi.org/10.1093/schbul/sbw183.
Kato, T.A., Monji, A., Mizoguchi, Y., Hashioka, S., Horikawa, H., Seki, Y., Kasai, M., Utsumi, H., Kanba, S., 2011. Anti-Inflammatory properties of antipsychotics via microglia modulations: are antipsychotics a “fire extinguisher” in the brain of schizophrenia? Mini Rev. Med. Chem. 11, 565–574.
Kowalski, J., Blada, P., Kucia, K., Madej, A., Herman, Z.S., 2001. Neuroleptics normalize increased release of interleukin-1β and tumor necrosis factor-α from monocytes in schizophrenia. Schizophr. Res. 50 (3), 169–175. https://doi.org/10.1016/S0920-9964(00)00156-0.
Krause, D.L., Wagner, J.K., Wildenauer, A., Matz, J., Weidinger, E., Riedel, M., Obermeier, M., Gruber, R., Schwarz, M., Müller, N., 2012. Intracellular monocytic cytokine levels in schizophrenia show an alteration of IL-6. Eur. Arch. Psychiatry Clin. Neurosci. https://doi.org/10.1007/s00406-012-0290-2.
Leone, C., Le Pavec, G., Même, W., Porcheray, F., Samah, B., Dormont, D., Gras, G., 2006. Characterization of human monocyte-derived microglia-like cells. Glia 54 (3), 183–192. https://doi.org/10.1002/glia.20372.
Lewitus, G., Konefal, S., Greenhalgh, A., Pribiag, H., Augereau, K., Stellwagen, D., 2016. Microglial TNF-α suppresses cocaine-induced plasticity and behavioral sensitization. Neuron. https://doi.org/10.1016/j.neuron.2016.03.030.
Liao, Y., Smyth, G.K., Shi, W., 2014. featureCounts: an efficient general purpose program for assigning sequence reads to genomic features. Bioinformatics 30, 923–930. https://doi.org/10.1093/bioinformatics/btt656.
Mandl, M., Schmitz, S., Weber, C., Hristov, M., 2014. Characterization of the cd14+ +cd16+ monocyte population in human bone marrow. PLoS One. https://doi.org/10.1371/journal.pone.0112140.
Mattei, D., Ivanov, A., Ferrai, C., Jordan, P., Guneykaya, D., Buonfiglioli, A., Schaafsma, W., Przanowski, P., Deuther-Conrad, W., Brust, P., Hesse, S., Patt, M., Sabri, O., Ross, T.L., Eggen, B.J.L., Boddeke, E.W.G.M., Kaminska, B., Beule, D., Pombo, A., Kettenmann, H., Wolf, S.A., 2017. Maternal immune activation results in complex microglial transcriptome signature in the adult offspring that is reversed by minocycline treatment. Transl Psychiatry 7, e1120. https://doi.org/10.1038/tp.2017.80.
Nowicka, M., Krieg, C., Weber, L.M., Hartmann, F.J., Guglietta, S., Becher, B., Levesque, M.P., Robinson, M.D., 2017. CyTOF workflow: differential discovery in high-throughput high-dimensional cytometry datasets. F1000Res. https://doi.org/10.12688/f1000research.11622.2.
Ohgidani, M., Kato, T.A., Setoyama, D., Sagata, N., Hashimoto, R., Shigenobu, K., Yoshida, T., Hayakawa, K., Shimokawa, N., Miura, D., Utsumi, H., Kanba, S., 2015. Direct induction of ramified microglia-like cells from human monocytes: Dynamic microglial dysfunction in Nasu-Hakola disease. Sci. Rep. 4. https://doi.org/10.1038/srep04957.
Ormel, P.R.P.R., van Mierlo, H.C.H.C., Litjens, M., Van Strien, M.E., Hol, E.M.E.M., Kahn, R.S.R.S., de Witte, L.D.L.D., 2017. Characterization of macrophages from schizophrenia patients. NPJ Schizophr. 3, 41. https://doi.org/10.1038/s41537-017-0042-4.
Ormel, P.R., Vieira de Sá, R., van Bodegraven, E.J., Karst, H., Harschnitz, O., Sneeboer, M.A.M., Johansen, L.E., van Dijk, R.E., Scheefhals, N., Berdenis van Berlekom, A., Ribes Martínez, E., Kling, S., MacGillavry, H.D., van den Berg, L.H., Kahn, R.S., Hol, E.M., de Witte, L.D., Pasterkamp, R.J., 2018. Microglia innately develop within cerebral organoids. Nat. Commun. 9, 4167. https://doi.org/10.1038/s41467-018-06684-2.
Patir, A., Shih, B., McColl, B.W., Freeman, T.C., 2019. A core transcriptional signature of human microglia: Derivation and utility in describing region-dependent alterations associated with Alzheimer's disease. Glia. https://doi.org/10.1002/glia.23572.
Ryan, K.J., White, C.C., Patel, K., Xu, J., Olah, M., Replogle, J.M., Frangieh, M., Cimpean, M., Winn, P., McHenry, A., Kaskow, B.J., Chan, G., Cuerdon, N., Bennett, D.A., Boyd, J.D., Imitola, J., Elyaman, W., De Jager, P.L., Bradshaw, E.M., 2017. A human microglia-like cellular model for assessing the effects of neurodegenerative disease gene variants. Sci. Transl. Med. 9, eaai7635. https://doi.org/10.1126/scitranslmed.aai7635.
Sekar, A., Bialas, A.R., de Rivera, H., Davis, A., Hammond, T.R., Kamitaki, N., Tooley, K., Presumey, J., Baum, M., Van Doren, V., Genovese, G., Rose, S.A., Handsaker, R.E., Daly, M.J., Carroll, M.C., Stevens, B., McCarroll, S.A., McCarroll, S.A., 2016. Schizophrenia risk from complex variation of complement component 4. Nature 530, 177–183. https://doi.org/10.1038/nature16549.
Sellgren, C.M., Gracias, J., Watmuff, B., Biag, J.D., Thanos, J.M., Whittredge, P.B., Fu, T., Worringer, K., Brown, H.E., Wang, J., Kaykas, A., Karmacharya, R., Goold, C.P., Sheridan, S.D., Perlis, R.H., 2019. Increased synapse elimination by microglia in schizophrenia patient-derived models of synaptic pruning. Nat. Neurosci. 22, 374–385. https://doi.org/10.1038/s41593-018-0334-7.
Skene, N.G., Bryois, J., Bakken, T.E., Breen, G., Crowley, J.J., Gaspar, H.A., Giusti-Rodriguez, P., Hodge, R.D., Miller, J.A., Muñoz-Manchado, A.B., O'Donovan, M.C., Owen, M.J., Pardiñas, A.F., Ryge, J., Walters, J.T.R., Linnarsson, S., Lein, E.S., Sullivan, P.F., Hjerling-Leffler, J., Hjerling-Leffler, J., 2018. Genetic identification of brain cell types underlying schizophrenia. Nat. Genet. 50, 825–833. https://doi.org/10.1038/s41588-018-0129-5.
Sneeboer, M.A.M., Snijders, G.J.L.J., Berdowski, W.M., Fernández-Andreu, A., van Mierlo, H.C., Berdenis van Berlekom, A., Litjens, M., Kahn, R.S., Hol, E.M., de Witte, L.D., 2019. Microglia in post-mortem brain tissue of patients with bipolar disorder are not immune activated. Transl. Psychiatry 9. https://doi.org/10.1038/s41398-019-0490-x.
Stellwagen, D., Malenka, R.C., 2006. Synaptic scaling mediated by glial TNF-α. Nature. https://doi.org/10.1038/nature04671.
Stevens, B., Allen, N.J., Vazquez, L.E., Howell, G.R., Christopherson, K.S., Nouri, N., Micheva, K.D., Mehalow, A.K., Huberman, A.D., Stafford, B., Sher, A., Litke, A.M., Lambris, J.D., Smith, S.J., John, S.W.M., Barres, B.A., 2007. The classical complement cascade mediates CNS synapse elimination. Cell 131, 1164–1178. https://doi.org/10.1016/j.cell.2007.10.036.
Tay, T.L., Béchade, C., D'Andrea, I., St-Pierre, M.-K., Henry, M.S., Roumier, A., Tremblay, M.-E., 2017. Microglia Gone Rogue: Impacts on Psychiatric Disorders across the Lifespan. Front. Mol. Neurosci. 10, 421. https://doi.org/10.3389/fnmol.2017.00421.
Upthegrove, R., Manzanares-Teson, N., Barnes, N.M., 2014. Cytokine function in medication-naive first episode psychosis: A systematic review and meta-analysis. Schizophr. Res. 155 (1-3), 101–108. https://doi.org/10.1016/j.schres.2014.03.005.
Van Gassen, S., Callebaut, B., Van Helden, M.J., Lambrecht, B.N., Demeester, P., Dhaene, T., Saeys, Y., 2015. FlowSOM: Using self-organizing maps for visualization and interpretation of cytometry data. Cytom. Part A. https://doi.org/10.1002/cyto.a.22625.
van Mierlo, H.C., Schot, A., Boks, M.P.M., de Witte, L.D., 2020. The association between schizophrenia and the immune system: Review of the evidence from unbiased 'omic-studies'. Schizophr. Res. https://doi.org/10.1016/j.schres.2019.05.028.
Werneburg, S., Feinberg, P.A., Johnson, K.M., Schafer, D.P., 2017. A microglia-cytokine axis to modulate synaptic connectivity and function. Curr. Opin. Neurobiol. https://doi.org/10.1016/j.conb.2017.10.002.